Chapter 24

Fundamental Limitations in MIMO Control

Arguably, the best way to learn about real design issues is to become involved in practical applications. We hope that the reader gained some feeling for the lateral thinking that is typically needed in most real-world problems, from reading the various case studies that we have presented.

In this chapter, we will adopt a more abstract stance and extend the design insights on Chapters 8 and 9 to the MIMO case.

It was shown in Chapters 8 and 9 that the open-loop properties of a SISO plant impose fundamental and unavoidable constraints on the closed-loop characteristics that are achievable. For example, we have seen that, for a one-degree-of-freedom loop, a double integrator in the open-loop transfer function implies that the integral of the error due to a step reference change must be zero. We have also seen that real RHP zeros necessarily imply undershoot in the response to a step reference change.

As might be expected, similar concepts apply to multivariable systems. However, whereas in SISO systems one has only the frequency (*or time*) axis along which to deal with the constraints, in MIMO systems there is also a spatial dimension: one can trade-off limitations between different outputs as well as on a frequency-by-frequency basis. This means that it is also necessary to account for the interactions between outputs, rather than simply being able to focus on one output at a time.

In terms of the *sensitivity dirt* concept introduced in Chapter 9, in MIMO systems we can spread this *dirt* in both the frequency dimension as well as the spatial dimension (*i.e. amongst different outputs*). This idea is captured in the cartoon on the next slide.

Multivariable Case

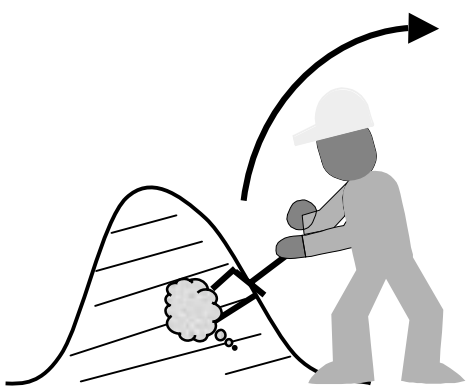

Sensitivity dirt

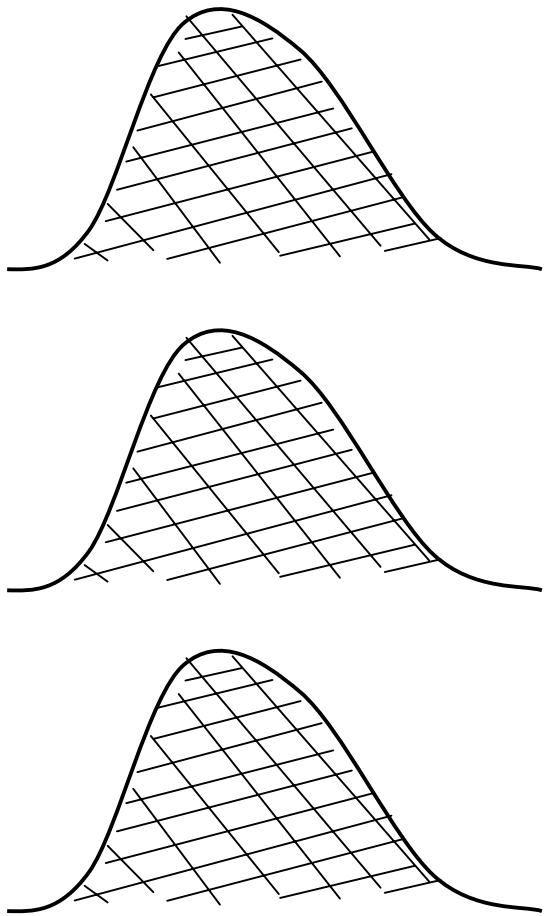

Multiple piles

Closed-Loop Transfer Function

We consider the MIMO loop of the form shown below.

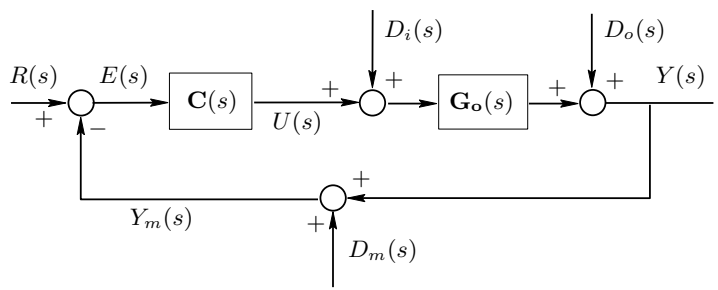

Figure 24.1: *MIMO Feedback loop*

We describe the plant model $\mathbf{G_o}(s)$ and the controller $\mathbf{C}(s)$ in LMFD and RMFD form as

$$\mathbf{G_o}(s) = \mathbf{G_{oN}}(s)[\mathbf{G_{oD}}(s)]^{-1} = \left[\, \overline{\mathbf{G}}_{\mathbf{oD}}(s)\right]^{-1} \overline{\mathbf{G}}_{\mathbf{oN}}(s)$$

$$\mathbf{C}(s) = \mathbf{C_N}(s)[\mathbf{C_D}(s)]^{-1} = \left[\, \overline{\mathbf{C}}_{\mathbf{D}}(s)\right]^{-1} \overline{\mathbf{C}}_{\mathbf{N}}(s)$$

For closed-loop stability, it is necessary and sufficient that the Matrix $\mathbf{A_{cl}}(s)$ be stably invertible, where

$$\mathbf{A_{cl}}(s) \triangleq \overline{\mathbf{G}}_{\mathbf{oD}}(s)\mathbf{C_D}(s) + \overline{\mathbf{G}}_{\mathbf{oN}}(s)\mathbf{C_N}(s)$$

For the purpose of the analysis in this chapter, we will continue working under the assumption that the MIMO plant is square, i.e., its model is an $m \times m$ transfer function matrix. We also assume that $\mathbf{G_o}(s)$ is nonsingular for almost all s and, in particular, that $\det \mathbf{G_o}(0) \neq 0$.

For future use, we denote the i^{th} column of $\mathbf{S_o}(s)$ as $[\mathbf{S_o}(s)]_{*i}$ and the k^{th} row of $\mathbf{T_o}(s)$ as $[\mathbf{T_o}(s)]_{k*}$; so

$$\mathbf{S_o}(s) = \begin{bmatrix}[\mathbf{S_o}(s)]_{*1} & [\mathbf{S_o}(s)]_{*2} & \cdots & [\mathbf{S_o}(s)]_{*m}\end{bmatrix}; \qquad \mathbf{T_o}(s) = \begin{bmatrix}[\mathbf{T_o}(s)]_{1*} \\ [\mathbf{T_o}(s)]_{2*} \\ \cdots \\ [\mathbf{T_o}(s)]_{m*}\end{bmatrix}$$

From Chapter 20, we recall that good nominal tracking is, as in the SISO case, connected to the issue of having low sensitivity in certain frequency bands. Upon examining this requirement, we see that it can be met if we can make

$$[\mathbf{I} + \mathbf{G_o}(j\omega)\mathbf{C_o}(j\omega)]^{-1}\mathbf{G_o}(j\omega)\mathbf{C_o}(j\omega) \approx \mathbf{I}$$

for all ω in the frequency bands of interest.

MIMO Internal Model Principle

In SISO control design, a key design objective is usually to achieve zero steady-state errors for certain classes of references and disturbances. However, we have also seen that this requirement can produce secondary effects on the transient behavior of these errors. In MIMO control design, similar features appear.

In Chapter 20, we showed that, to achieve zero steady-state errors to step reference inputs on each channel, we require that

$$\mathbf{T_o}(0) = \mathbf{I} \Longleftrightarrow \mathbf{S_o}(0) = \mathbf{0}$$

We have seen earlier in the book that a sufficient condition to obtain this result is that we can write the controller as

$$\mathbf{C}(s) = \frac{1}{s}\overline{\mathbf{C}}(s) \qquad \text{where} \qquad \det(\overline{\mathbf{C}}(0)) \neq 0$$

This is usually achieved in practice by placing one integrator in each error channel.

The Cost of the Internal Model Principle

As in the SISO case, the Internal Model Principle comes at a cost. As an illustration, the following result extends a SISO result (*namely Lemma 8.1 from Chapter 8*) to the multivariable case.

Lemma 24.1: If zero steady-state errors are required to a ramp reference input on the r^{th} channel, then it is necessary that

$$\lim_{s \to 0} \frac{1}{s} [\mathbf{S_o}(s)]_{*r} = 0$$

and, as a consequence, in a one-d.o.f. loop,

$$\int_0^\infty e_i^r(t)dt = 0 \qquad i = 1, 2, \ldots, m$$

where $e_i^r(t)$ denotes the error in the i^{th} channel resulting from a step reference input on the r^{th} channel.

It is interesting to note the essentially multivariable nature of the above result. The integral of all channel errors is zero, in response to a step reference in only one channel. We will establish similar multivariable results for the case of RHP poles are zeros.

Furthermore, Lemma 24.1 shows that all components of the MIMO plant output will overshoot their stationary values when a step reference change occurs on the r^{th} channel.

RHP Poles and Zeros

In the case of SISO plants, we found that performance limitations are intimately connected to the presence of open-loop RHP poles and zeros. We shall find that this is also true in the MIMO case. As a prelude to developing these results, we first review the appropriate definitions of poles and zeros.

Consider the plant model $\mathbf{G_o}(s)$. We recall that z_0 is a zero of $\mathbf{G_o}(s)$, with corresponding left directions $h_1^T, h_2^T, \ldots, h_{\mu_z}^T$, if

$$\det(\mathbf{G_{oN}}(z_o)) = 0 \quad \text{and} \quad h_i^T(\mathbf{G_{oN}}(z_o)) = 0 \quad i = 1, 2, \ldots, \mu_z$$

Similarly, we say that η_0 is a pole of $\mathbf{G_o}(s)$, with corresponding right directions $g_1, g_2, \ldots, g_{\mu p}$, if

$$\det(\overline{\mathbf{G}}_{\mathbf{oD}}(\eta_o)) = 0 \quad \text{and} \quad (\overline{\mathbf{G}}_{\mathbf{oD}}(\eta_o))g_i = 0 \quad i = 1, 2, \ldots, \mu_p$$

MIMO Interpolation Constraints

If we now assume that z_0 and η_0 are not canceled by the controller, then the following lemma holds.

Lemma 24.2: With z_0 and η_0 defined as above,

$$\begin{aligned}
\mathbf{S_o}(\eta_o)g_i &= 0 && i = 1, 2, \ldots \mu_p \\
\mathbf{T_o}(\eta_o)g_i &= g_i && i = 1, 2, \ldots \mu_p \\
h_i^T\mathbf{T_o}(z_o) &= 0 && i = 1, 2, \ldots \mu_z \\
h_i^T\mathbf{S_o}(z_o) &= h_i^T && i = 1, 2, \ldots \mu_z
\end{aligned}$$

We see that, as in the SISO case, open-loop poles (*i.e. the poles of* $\mathbf{G_o}(s)\mathbf{C}(s)$) become zeros of $\mathbf{S_o}(s)$, and open-loop zeros (*i.e. the zeros of* $\mathbf{G_o}(s)\mathbf{C}(s)$) become zeros of $\mathbf{T_o}(s)$.

Time-Domain Constraints

We saw in Chapter 8 for the SISO case that the presence of RHP poles and zeros had certain implications for the time responses of closed-loop systems. We have the following MIMO version of Lemma 8.3.

Lemma 24.3: Consider a MIMO feedback control loop having stable closed-loop poles located to the left of $-\alpha$ for some $\alpha > 0$. Also, assume that zero steady-state error occurs for reference step inputs in all channels. Then, for a plant zero z_0 with left directions $h_1^T, h_2^T, \ldots, h_{\mu z}^T$ and a plant pole η_0 with right directions $g_1, g_2, \ldots, g_{\mu p}$ satisfying $\Re(z_0) > -\alpha$ and $\Re(\eta_0) > -\alpha$, we have the following:

(*i*) For a positive unit reference step on the r^{th} channel,

$$\int_0^\infty h_i^T e(t) e^{-z_o t} dt = \frac{h_{ir}}{z_o}; \qquad i = 1, 2, \ldots, \mu_z$$

where h_{ir} is the r^{th} component of h_i.

(*ii*) For a (*positive or negative*) unit-step output disturbance in direction g_i, $i = 1, 2, \ldots, \mu_p$, the resulting error, $e(t)$, satisfies

$$\int_0^\infty e(t)e^{-\eta_o t}dt = 0$$

(*iii*) For a (*positive or negative*) unit reference step in the r^{th} channel, and provided that z_0 is in the RHP,

$$\int_0^\infty h_i^T y(t) e^{-z_o t} dt = 0; \qquad i = 1, 2, \ldots, \mu_z$$

Proof: See the book.

Comparing the above Lemma with Lemma 8.3 clearly shows the multivariable nature of these constraints. For example part (*ii*) holds for disturbances coming from a particular direction. Also, part (*i*) applies to particular combinations of the errors. Thus, the undershoot property can (*sometimes*) be shared amongst different error channels, depending on the directionality of the zeros.

Example

Quadruple-tank apparatus continued.

Consider again the quadruple-tank apparatus. We recall from our early study of this example, that for the case $\gamma 1 = 0.43$, $\gamma 2 = 0.34$, there is a nonminimum-phase zero at $z_0 = 0.0229$. The associated left zero direction is approximately [1 -1].

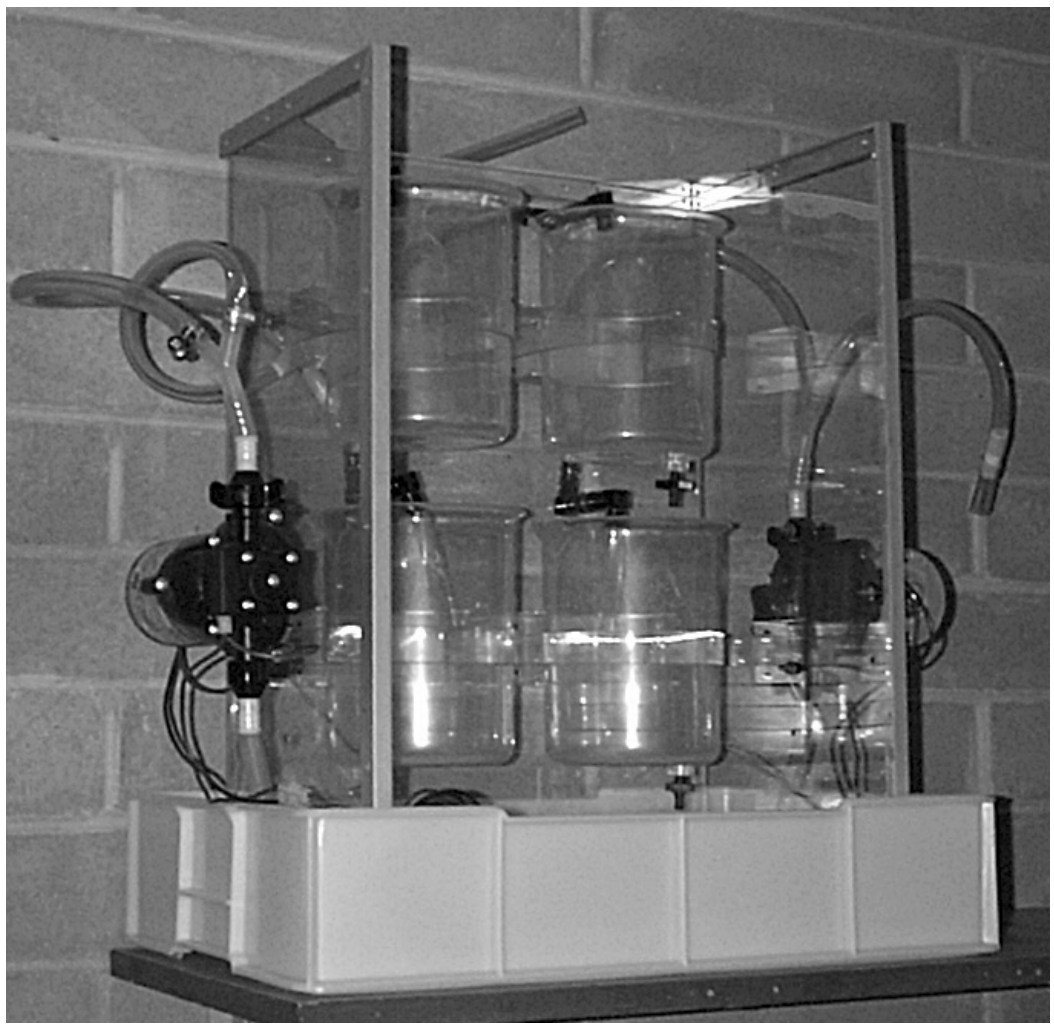

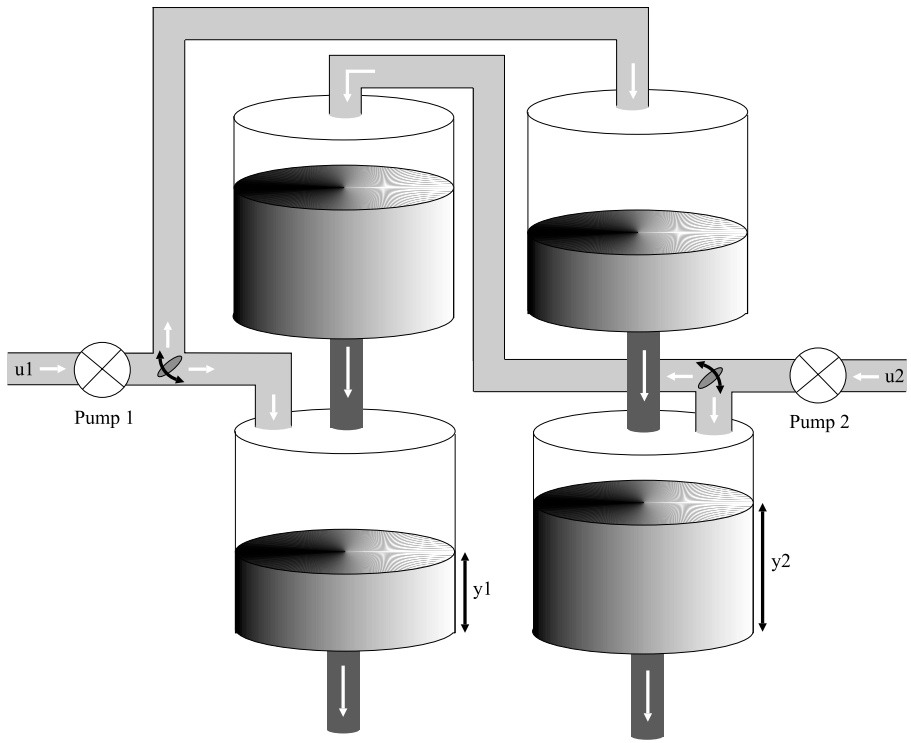

Hence, from Lemma 24.3 we have

$$\int_0^\infty (y_1(t) - y_2(t))e^{-z_o t}dt = 0$$
$$\int_0^\infty (e_1(t) - e_2(t))e^{-z_o t}dt = \frac{(-1)^{i-1}}{z_o}$$

for a unit step in the i^{th} channel reference.

The zero in this case is an *interaction zero*; hence, we do not necessarily get undershoot in the response However, there are constraints on the extent of interaction that must occur. This explains the high level of interaction observed in the next slide.

We actually see that there are two ways one can deal with this constraint.

Simulation of Closed Loop Responses

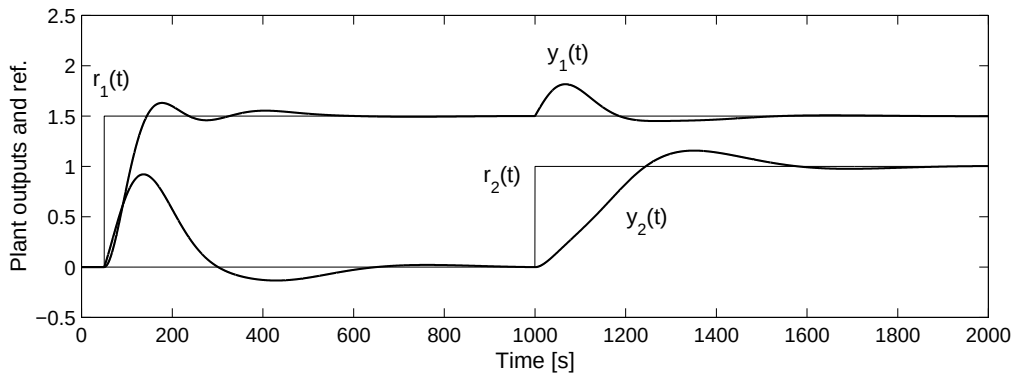

(*i*) If we allow coupling in the final response, then we can spread the constraint between outputs; i.e., we can satisfy the integral constraints by having $y_2(t)$, and hence $e_2(t)$, respond when a step is applied to channel 1 reference, and vice-versa. This might allow us to avoid undershoot, at the expense of having interaction. The amount of interaction needed grows as the bandwidth increases beyond z_0.

(*ii*) If we design and achieve (*near*) decoupling, then only one of the outputs can be nonzero after each individual reference changes.

This implies that undershoot must occur in this case. Also, we see that undershoot will occur in both channels (*i.e.*, *the effect of the single RHP zero now influences both channels*). This is an example of *spreading* resulting from dynamic decoupling.

General comments on effect of decoupling

It is interesting to see the impact of dynamic decoupling on the MIMO integral constraint:

$$\int_0^\infty h_i^T e(t) e^{-z_o t} dt = \frac{h_{ir}}{z_o}; \qquad i = 1, 2, \ldots, \mu_z$$

If we can achieve a design with the decoupling property (*a subject to be analyzed in greater depth in Chapter 26*), then it necessarily follows, that for a reference step in the r^{th} channel, there will be no effect on the other channels:

$$e_k(t) = 0 \qquad \text{for} \quad \forall k \neq r, \qquad \forall t > 0$$

Then the integral constraint reduces to the following result:

$$\int_0^\infty h_{ir} e_r(t) e^{-z_o t} dt = \frac{h_{ir}}{z_o}; \qquad i = 1, 2, \ldots, \mu_z$$

or, for $h_{ir} \neq 0$,

$$\int_0^\infty e_r(t) e^{-z_o t} dt = \frac{1}{z_o}$$

which is exactly the constraint applicable to the SISO case.

We thus conclude that dynamic decoupling removes the possibility of sharing the *zero constraint* amongst different error channels. This is heuristically reasonable. We also see that one zero can effect multiple channels under a decoupled design.

The only time that a zero does not *spread its influence* over many channels is when the corresponding zero direction has only one nonzero component. We then say that the corresponding zero direction is *canonical*.

Example 24.2

Consider the following transfer function:

$$\mathbf{G_o}(s) = \begin{bmatrix} \dfrac{s-1}{(s+1)^2} & \dfrac{2(s-1)}{(s+1)^2} \\ \dfrac{1}{(s+1)^2} & \dfrac{\epsilon}{(s+1)^2} \end{bmatrix}$$

We see that $z_0 = 1$ is a zero with direction $h_1{}^T = [1 \quad 0]$. We see that is a canonical direction. In this case, the integral constraint becomes

$$\int_0^\infty [1 \quad 0]^T e(t) e^{-t} dt = \int_0^\infty e_1(t) e^{-t} dt = \frac{1}{z_o} = 1$$

for a step input on the first channel. Note that, in this case, this is the same as the SISO case. Thus the effect of the single zero is not *spread* over multiple channels, i.e. there is no additional cost to decoupling in this case.

However, if we instead consider the plant

$$\mathbf{G_o}(s) = \begin{bmatrix} \dfrac{s-1}{(s+1)^2} & \dfrac{1}{(s+1)^2} \\ \dfrac{2(s-1)}{(s+1)^2} & \dfrac{\epsilon}{(s+1)^2} \end{bmatrix}$$

then the situation changes significantly.

In this case, $z_0 = 1$ is a zero with direction $h_1{}^T = [\,\epsilon \;\; -1]$. We see that is a non-canonical direction. Thus the integral constant gives for a step reference in the first channel that

$$\int_0^\infty [\epsilon \ -1]^T e(t)e^{-t}dt = \int_0^\infty (\epsilon e_1(t) - e_2(t))e^{-t}dt = \frac{\epsilon}{z_o} = \epsilon$$

and for a step reference in the second channel that

$$\int_0^\infty (\epsilon e_1(t) - e_2(t))e^{-t}dt = \frac{-1}{z_o} = -1$$

If, on the other hand, we insist on dynamic decoupling, we obtain for a unit step reference in the first channel that

$$\int_0^\infty e_1(t)e^{-t}dt = \frac{1}{z_o} = 1$$

and for a step reference in the second channel that

$$\int_0^\infty e_2(t)e^{-t}dt = \frac{1}{z_o} = 1$$

Thus the effect of the zero has been *spread* by the decoupling design over the two channels.

Clearly, in this example, a small amount of coupling from channel 1 into channel 2 can be very helpful when $\epsilon \neq 0$.

The time-domain constraints explored above are also matched by frequency-domain constraints that are the MIMO extensions of the SISO results presented in Chapter 9. This is explored below.

Poisson Integral Constraints on MIMO Complementary Sensitivity

We will develop the MIMO versions of results presented in Section 9.5.

Note that the vector $\mathbf{T_o}(s)g_i$ can be premultiplied by a matrix $\mathbf{B_i}(s)$ to yield a vector $\tau_i(s)$:

$$\tau_i(s) = \mathbf{B_i}(s)\mathbf{T_o}(s)g_i = \begin{bmatrix} \tau_{i1}(s) \\ \tau_{i2}(s) \\ \vdots \\ \tau_{im}(s) \end{bmatrix}; \qquad i = 1, 2, \ldots, \mu_p$$

where $\mathbf{B_i}(s)$ is a diagonal matrix in which each diagonal entry $[\mathbf{B_i}(s)]_{jj}$, is a scalar inverse Blaschke product, constructed so that $\ln(\tau_{ij}(s))$ is an analytic function in the open RHP.

We also define a column vector $\overline{g}_i(s)$ as follows:

$$\overline{g}_i(s) = \mathbf{B_i}(s) g_i = \begin{bmatrix} [\mathbf{B_i}(s)]_{11} g_{i1}(s) \\ \vdots \\ [\mathbf{B_i}(s)]_{mm} g_{im}(s) \end{bmatrix} = \begin{bmatrix} \overline{g}_{i1}(s) \\ \vdots \\ \overline{g}_{im}(s) \end{bmatrix}$$

We next define a set of integers, ∇_i, corresponding to the indices of the nonzero elements of g_i:

$$\nabla_i = \{r | g_{ir} \neq 0\}; \qquad i = 1, 2, \ldots, \mu_p$$

We then have the following result:

Theorem 24.1 *Complementary sensitivity and unstable poles:*

Consider a MIMO system with an unstable pole located at $s = \eta_0 = \alpha + j\beta$ and having associated directions $g_1, g_2, \ldots, g_{\mu_p}$; then

(*i*)

$$\frac{1}{\pi}\int_{-\infty}^{\infty} \ln|[\mathbf{T_o}(j\omega)]_{r*} g_i| d\Omega(\eta_o, \omega) = \ln|B_{ir}(\eta_o) g_{ir}|; \qquad r \in \nabla_i; \qquad i = 1, 2, \ldots, \mu_p$$

(*ii*)

$$\frac{1}{\pi}\int_{-\infty}^{\infty} \ln|[\mathbf{T_o}(j\omega)]_{r*}g_i|d\Omega(\eta_o,\omega) \geq \ln|g_{ir}|; \qquad r \in \nabla_i; \qquad i = 1, 2, \ldots, \mu_p$$

where

$$d\Omega(\eta_o,\omega) = \frac{\alpha}{\alpha^2 + (\omega-\beta)^2}d\omega \Longrightarrow \int_{-\infty}^{\infty} d\Omega(\eta_o,\omega) = \pi$$

Proof: See the book.

Remark: Although the above result gives a precise conclusion, it is a constraint that depends on the controller. The result presented in the following corollary is independent of the controller.

Corollary: Consider Theorem 24.1; then the result can also be written as

$$\int_{-\infty}^{\infty} \ln |[\mathbf{T_o}(j\omega)]_{rr}| \, d\Omega(\eta_o, \omega) \geq \int_{-\infty}^{\infty} \ln \left| \frac{[\mathbf{T_o}(j\omega)]_{rr} g_{ir}}{\sum_{k \in \nabla} [\mathbf{T_o}(j\omega)]_{rk} g_{ik}} \right| d\Omega(\eta_o, \omega)$$

Poisson Integral Constraints on MIMO Sensitivity

When the plant has NMP zeros, a result similar to the one presented above can be established for the sensitivity function, $\mathbf{S_o}(s)$.

We first note that the vector $h_i^T \mathbf{S_o}(s)$ can be postmiultiplied by a matrix $\mathbf{B_i}'(s)$ to yield a vector $\upsilon_i(s)$:

$$\upsilon_i(s) = h_i^T \mathbf{S_o}(s)\mathbf{B_i'}(s) = \begin{bmatrix} \upsilon_{i1}(s) & \upsilon_{i2}(s) & \dots & \upsilon_{im}(s) \end{bmatrix}; \qquad i = 1, 2, \dots, \mu_z$$

where $\mathbf{B_i}'(s)$ is a diagonal matrix in which each diagonal entry, $[\mathbf{B_i}'(s)]_{jj}$, is a scalar inverse Blaschke product, constructed so that $\ln(\upsilon_{ij}(s))$ is an analytic function in the open RHP.

We also define a row vector $\overline{h}_i(s)$, where

$$\overline{h}_i(s) = h_i^T(s)\mathbf{B}_\mathbf{i}'(s) = \begin{bmatrix} h_{i1}^T(s)[\mathbf{B}_\mathbf{i}'(s)]_{11} \\ \vdots \\ h_{im}^T(s)[\mathbf{B}_\mathbf{i}'(s)]_{mm} \end{bmatrix} = \begin{bmatrix} \overline{h}_{i1}(s) & \dots & \overline{h}_{im}(s) \end{bmatrix}$$

We next define a set of integers ∇_i' corresponding to the indices of the nonzero elements of h_i:

$$\nabla_i' = \{r | h_{ir} \neq 0\}; \qquad i = 1, 2, \ldots, \mu_z$$

We then have the following result:

Theorem 24.2 *Sensitivity and NMP zeros:*

Consider a MIMO plant having a NMP zero at $s = z_0 = \gamma + j\delta$, which associated directions h_1^T, h_2^T, …, $h_{\mu_z}^T$; then the sensitivity in any control loop for that plant satisfies

(*i*)

$$\frac{1}{\pi}\int_{-\infty}^{\infty} \ln|h_i^T[\mathbf{S_o}(j\omega)]_{*r}|d\Omega(z_o,\omega) = \ln|h_{ir}[\mathbf{B_i'(z_o)}]_{rr}|; \qquad r \in \nabla_i'; \qquad i = 1, 2, \ldots, \mu_p$$

(*ii*)

$$\frac{1}{\pi}\int_{-\infty}^{\infty} \ln|h_i^T[\mathbf{S_o}(j\omega)]_{*r}|d\Omega(z_o,\omega) \geq \ln|h_{ir}|; \qquad r \in \nabla_i'; \qquad i = 1, 2, \ldots, \mu_p$$

where

$$d\Omega(z_o,\omega) = \frac{\gamma}{\gamma^2 + (\omega - \delta)^2}d\omega \Longrightarrow \int_{-\infty}^{\infty} d\Omega(z_o,\omega) = \pi$$

Proof: See the book.

Corollary: The result can also be written as

$$\int_{-\infty}^{\infty} \ln |[\mathbf{S_o}(j\omega)]_{rr}| \, d\Omega(z_o, \omega) \geq \int_{-\infty}^{\infty} \ln \left| \frac{h_{ir}[\mathbf{S_o}(j\omega)]_{rr}}{\sum_{k \in \nabla'} h_{ik}[\mathbf{S_o}(j\omega)]_{kr}} \right| d\Omega(z_o, \omega)$$

Interpretation

The above theorem shows that in MIMO systems, as is the case in SISO systems, there is a sensitivity trade-off along a frequency-weighted axis. Note also, that in the MIMO case, there is a spatial dimension (*i.e. multiple outputs*) aspect to the constraints. To explore the issue further, we consider the following lemma.

Lemma 24.2: Consider the l^{th} column ($l \in \nabla_i'$) in the case when the l^{th} sensitivity column, $[\mathbf{S_o}]_{*l}$, is considered. Furthermore, assume that some design specifications require that

$$|\mathbf{S_o}(j\omega)|_{kl} \leq \epsilon_{kl} \ll 1; \qquad \forall \omega \in [0, \omega_c]; k = 1, 2, \ldots, m$$

Then the following inequality must be satisfied:

$$\|[\mathbf{S_o}]_{ll}\|_\infty + \sum_{\substack{k=1 \\ k \neq l}}^{m} \left| \frac{h_{ik}}{h_{il}} \right| \|[\mathbf{S_o}]_{kl}\|_\infty \geq \left(\epsilon_{ll} + \sum_{\substack{k=1 \\ k \neq l}}^{m} \left| \frac{h_{ik}}{h_{il}} \right| \epsilon_{kl} \right)^{-\frac{\psi(\omega_c)}{\pi - \psi(\omega_c)}}$$

Where

$$\psi(\omega_c) = \int_o^{\omega_c} \left[\frac{\gamma}{\gamma^2 + (\omega - \delta)^2} + \frac{\gamma}{\gamma^2 + (\omega + \delta)^2} \right] d\omega$$

Proof: See the book.

These results are similar to those derived for SISO control loops, because we also obtain lower bounds for sensitivity peaks. Furthermore, these bounds grow with bandwidth requirements.

However, a major difference is that in the MIMO case the bound refers to a linear combination of sensitivity peaks. This combination is determined by the directions associated with the NMP zero under consideration.

An Industrial application: Sugar Mill

In this section, we consider the design of a controller for a typical industrial process. It has been chosen because it includes significant multivariable interactions, a nonself regulating nature, and nonminimum-phase behavior.

The sugar mill unit under consideration constitutes one of multiple stages in the overall process. A schematic diagram of the Mill Train is shown on the next slide.

Figure 24.2: *A sugar milling train*

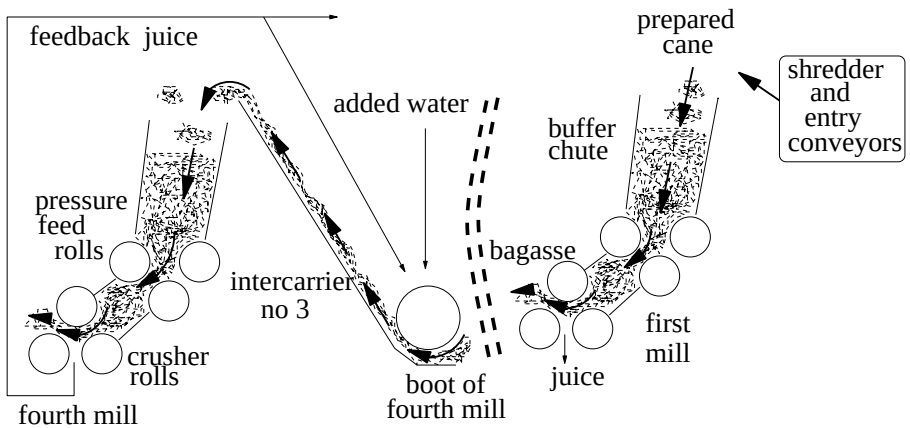

A single stage of this Milling Train is shown below:

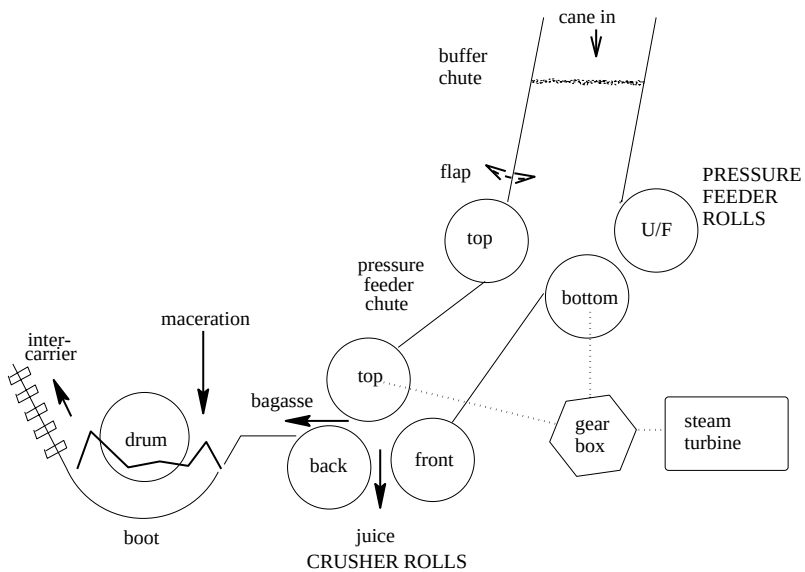

Figure 24.3: Single crushing mill

A photograph of the buffer chute and rolls is shown on the next slide.

For the purpose of maximal juice extraction, the process requires the control of two quantities: the buffer chute height, $h(t)$, and the mill torque, $\tau(t)$. For the control of these variables, the flap position, $f(t)$, and the turbine speed set-point $\omega(t)$, may be used. For control purposes, this plant can thus be modeled as a MIMO system with 2 inputs and 2 outputs. In this system, the main disturbance, $d(t)$, originates in the variable feed to the buffer chute.

In this example, regulation of the height in the buffer chute is less important for the process than regulation of the torque.

After applying phenomenological considerations and the performing of different experiments with incremental step inputs, a linearized plant model was obtained. The outcome of the modeling stage is below.

Figure 24.4: *Sugar mill linearized block model*

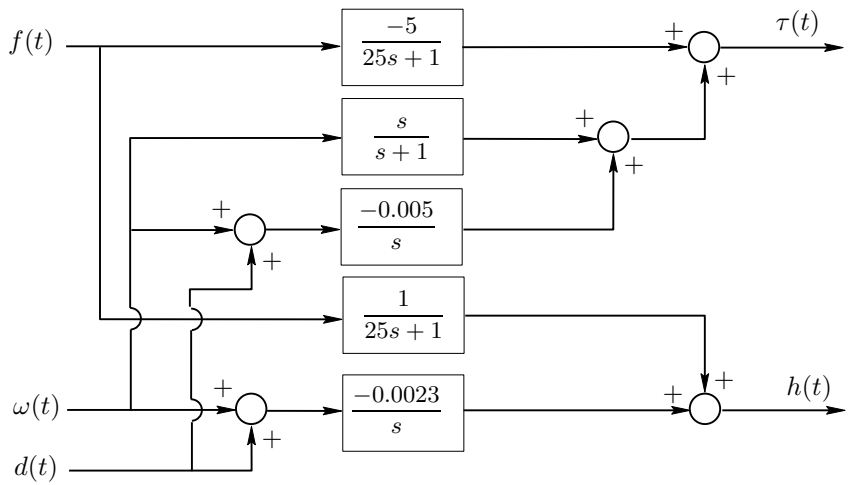

The nominal plant model in RMFD form, linking the inputs $f(t)$ and $\omega(t)$ to the outputs $\tau(t)$ and $h(t)$ is thus

$$\mathbf{G_o}(s) = \mathbf{G_{oN}}(s)[\mathbf{G_{oD}}(s)]^{-1}$$

where

$$\mathbf{G_{oN}}(s) = \begin{bmatrix} -5 & s^2 - 0.005s - 0.005 \\ 1 & -0.0023(s+1) \end{bmatrix}; \qquad \mathbf{G_{oD}}(s) = \begin{bmatrix} 25s+1 & 0 \\ 0 & s(s+1) \end{bmatrix}$$

We can now compute the poles and zeros of $\mathbf{G_o}(s)$. The poles of $\mathbf{G_o}(s)$ are the zeros of $\mathbf{G_{oD}}(s)$, i.e., (-1, -0.04, 0). The zeros of $\mathbf{G_o}(s)$ are the zeros of $\mathbf{G_{oN}}(s)$, i.e., the values of s that are roots of $\det(\mathbf{G_{oN}}(s)) = 0$; this leads to (-0.121, 0.137). Note that the plant model has a nonminimum-phase zero, located at $s = 0.137$.

We also have that

$$\mathbf{G_o}(0.137) = \begin{bmatrix} -1.13 & 0.084 \\ 0.226 & -0.0168 \end{bmatrix}$$

the direction associated with the NMP zero is given by

$$h^T = \begin{bmatrix} 1 & 5 \end{bmatrix}$$

Designs

Three designs were carried out and compared. These were:

(*i*) *A Decentralized SISO Design*

(*ii*) *Full Dynamic Decoupled Design*

(*iii*) *Triangular Decoupled Design.*

We leave the reader to follow the details of these designs in the book. We will simply summarize the results here.

SISO Design

Before attempting any MIMO design, we start by examining a SISO design using two separate PID controllers. In this design, we initially ignore the cross-coupling terms in the model transfer function $\mathbf{G_o}(s)$, and we carry out independent PID designs for the resulting two SISO models, i.e.

$$G_{11}(s) = \frac{-5}{25s+1}; \qquad \text{and} \qquad G_{22}(s)\frac{-0.0023}{s}$$

The final controllers obtained from this design were:

$$C_1(s) = -\frac{0.5s + 0.02}{s}; \qquad \text{and} \qquad C_2(s) = -\frac{20s^2 + 10s + 0.2}{s^2 + s}$$

To illustrate the limitations of this approach and the associated trade-offs, Figure 24.5 shows the performance of the loop under the resultant SISO-designed PID controllers.

In this simulation, the (*step*) references and disturbance were set as follows:

$$r_1(t) = \mu(t-1); \qquad r_2(t) = \mu(t-100); \qquad d(t) = -10\mu(t-250)$$

Figure 24.5: *Loop performance with SISO design*

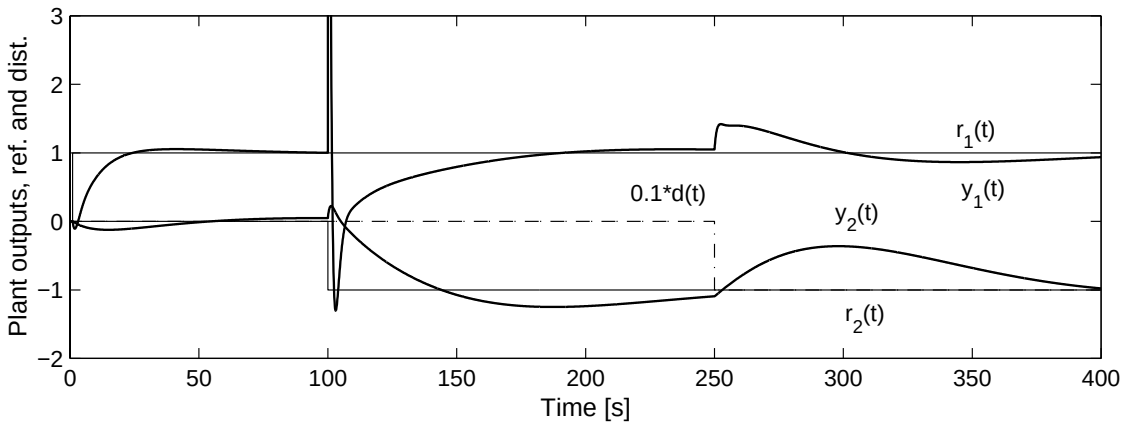

The following observations follow from the results above.

(*i*) Interaction between the loops is strong. In particular, we observe that a reference change in channel 2 (*height*) will induce strong perturbations of the output in channel 1 (*torque*).

(*ii*) Both outputs exhibit nonminimum-phase behavior. However, due to the design-imposed limitation on the bandwidth, this is not very strong in either of the outputs in response to a change in its own reference. Notice however, that the transient in y_1 in response to a reference change in r_2 is - because of the interaction neglected in the design - clearly of nonminimum phase.

(*iii*) The effects of the disturbance on the outputs show mainly low-frequency components. This is due to the fact that abrupt changes in the feed rate are filtered out by the buffer.

MIMO Designs

We now consider a full MIMO design. We begin by analyzing the main issues that will affect the MIMO design. They can be summarized as follows:

(*i*) The compensation of the input disturbance requires that integration be included in the controller to be designed.

(*ii*) To ensure internal stability, the NMP zero must not be canceled by the controller. Thus, $\mathbf{C}(s)$ should not have poles at $s = 0.137$.

(*iii*) In order to avoid the possibility of input saturation, the bandwidth should be limited. We will work in the range of 0.1-0.2[*rad/s*].

(*iv*) The location of the NMP zero suggests that the dominant mode in the channel(s) affected by that zero should not be faster than $e^{-0.137t}$. Otherwise, responses to step reference and step input disturbances will exhibit significant undershoot.

(*v*) The left direction, $h^T = [1 \quad 5]$, associated with the NMP zero is not a canonical direction. Hence, if dynamic decoupling is attempted, the NMP zero will affect both channels.

MIMO Design. Dynamic Decoupling

We first produce a decoupling design.

The appropriate controller in this case is given by

$$\mathbf{C}(s) = \begin{bmatrix} \dfrac{(25s+1)n_{11}(s)M_{11}(s)}{d^-(s)d^+(s)} & \dfrac{(25s+1)n_{12}(s)M_{22}(s)}{d^-(s)d^+(s)} \\ \dfrac{sn_{21}M_{11}(s)}{d^-(s)d^+(s)} & \dfrac{sn_{22}(s)M_{22}(s)}{d^-(s)d^+(s)} \end{bmatrix}$$

C(s) should not have poles at $s = 0.137$, so the polynomial $d^+(s)$ should be canceled in the four fraction matrix entries. This implies that

$$M_{11}(0.137) = M_{22}(0.137) = 0$$

Furthermore, we need to completely compensate the input disturbance, so we require integral action in the controller (*in addition to the integral action in the plant*). We thus make the following choices

$$M_{11}(s) = \frac{(s - 0.137)p_{11}(s)}{s^2 l_{11}(s)}; \qquad \text{and} \qquad M_{22}(s) = \frac{(s - 0.137)p_{22}(s)}{s^2 l_{22}(s)}$$

where $p_{11}(s)$, $l_{11}(s)$, $l_{22}(s)$, and $p_{22}(s)$ are chosen by using polynomial pole-placement techniques.

With these values, the controller is calculated. A simulation was run with this design and with the same conditions as for the decentralized PID case, i.e.,

$$r_1(t) = \mu(t-1); \qquad r_2(t) = \mu(t-100); \qquad d(t) = -10\mu(t-250)$$

The results are shown on the next slide.

Figure 24.6: *Loop performance with dynamic decoupling design*

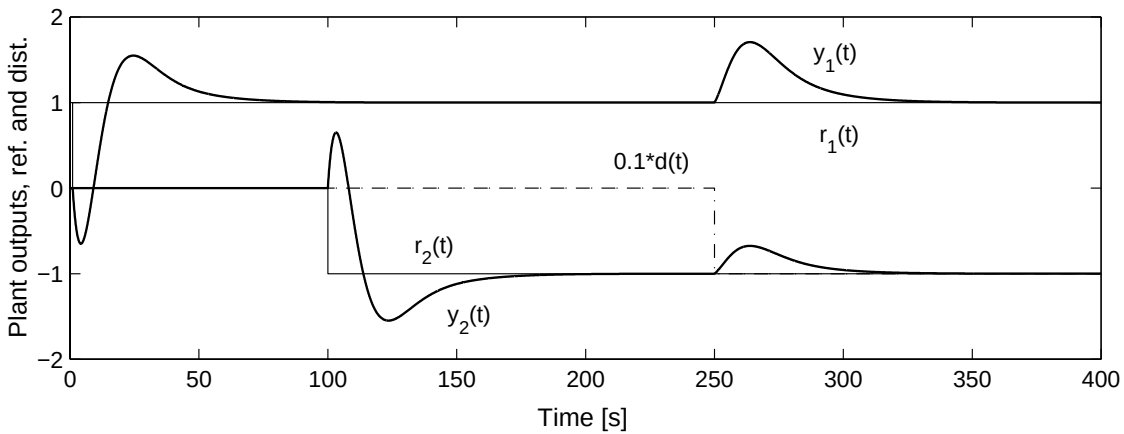

The results shown above confirm the two key issues underlying this design strategy: the channels are dynamically decoupled, and the NMP zero affects both channels.

MIMO Design. Triangular Decoupling

Next we aim for a triangular closed loop transfer function.

The resultant triangular structure will have the form

$$\mathbf{M}(s) = \mathbf{G_o}(s)\mathbf{C}(s) = \begin{bmatrix} M_{11}(s) & 0 \\ M_{21}(s) & M_{22}(s) \end{bmatrix}$$

This leads to the complementary sensitivity

$$\mathbf{T_o}(s) = \begin{bmatrix} T_{11}(s) & T_{12}(s) \\ T_{21}(s) & T_{22}(s) \end{bmatrix} = \begin{bmatrix} \dfrac{M_{11}(s)}{1+M_{11}(s)} & 0 \\ \dfrac{M_{21}(s)}{(1+M_{11}(s))(1+M_{22}(s))} & \dfrac{M_{22}(s)}{1+M_{22}(s)} \end{bmatrix}$$

The final controller is

$$C_{21}(s) = \frac{0.15(s+1)}{s(s+0.121)}$$

$$C_{11}(s) = \frac{-0.0058(25s+1)(s+0.0678)}{s^2(s+0.121)}$$

$$C_{12}(s) = \frac{-(25s+1)(s^2-0.005s-0.005)(0.4715s+0.0146)}{s^2(s+0.121)(s+0.8715)}$$

$$C_{22}(s) = \frac{-5(s+1)(0.4715s+0.0146)}{s(s+0.121)(s+0.8715)}$$

Unit step references and a unit step disturbance were applied, as follows:

$$r_1(t) = \mu(t-1); \qquad r_2(t) = -\mu(t-100); \qquad d(t) = -10\mu(t-250)$$

The results are shown on the next slide.

Figure 24.7: *Loop performance with triangular design*

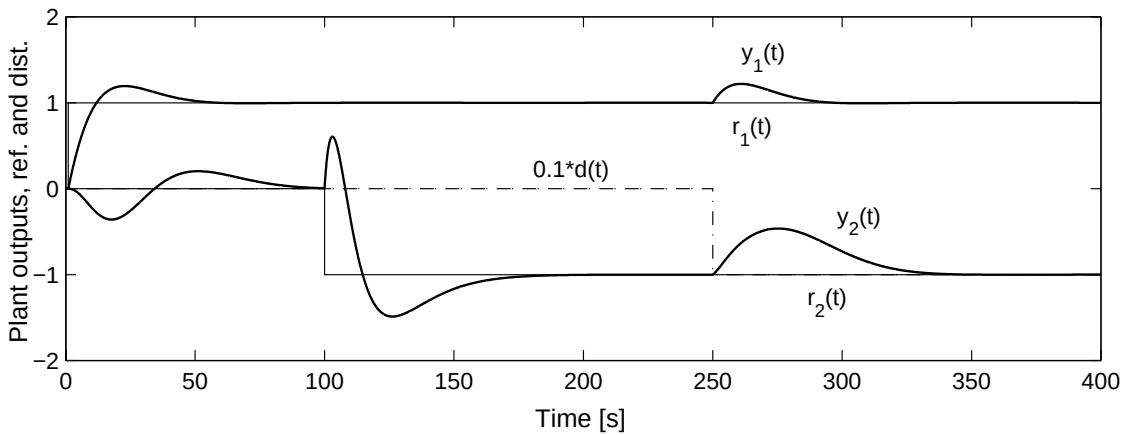

The following observations can be made about the above results:.

(*i*) The output of channel 1 is now unaffected by changes in the reference for channel 2. However, the output of channel 2 is affected by changes in the reference for channel 1. The asymmetry is consistent with the choice of a lower-triangular complementary sensitivity, $\mathbf{T_o}(s)$.

(ii) The nonminimum-phase behavior is evident in channel 2 but does not show up in the output of channel 1. This has also been achieved by choosing a lower-triangular $\mathbf{T_o}(s)$; that is, the open-loop NMP zero is a canonical zero of the closed-loop.

(*iii*) The transient compensation of the disturbance in channel 1 has also been improved with respect to the fully decoupled loop.

(*iv*) The step disturbance is completely compensated in steady state. This is due to the integral effect in the control for both channels.

(*v*) The output of channel one exhibits significant overshoot (*around* 20%). This was predicted for any loop having a double integrator.

Nonsquare Systems

In most of the above treatment, we have assumed equal number of inputs and outputs. However, in practice, there are either excess inputs (*fat systems*) or extra measurements (*tall systems*). We briefly discuss these two scenarios below.

Excess inputs

Say we have *m* inputs and p outputs, where $m > p$. In broad terms, the design alternatives can be characterized under four headings:

(a) *Squaring up*

Because we have extra degrees of freedom in the input, it is possible to control extra variables (*even though they need not be measured*). One possible strategy is to use an observer to estimate the missing variables.

(b) *Coordinated control*

Another, and very common, situation, is where p inputs are chosen as the primary control variables, but other variables from the remaining m - p inputs are used in some fixed, or possibly dynamic, relationships to the primary controls.

(c) *Soft load sharing*

It one decides to simply control the available measurements, then one can share the load of achieving this control between the excess inputs. This can be achieved via various optimization approaches (*e.g.*, *quadratic*).

(d) *Hard load sharing*

It is often the case that one has a subset of the inputs (*say of dimension p*) that is a preferable choice from the point of view of precision or economics, but that these have limited amplitude or authority. In this case, other inputs can be called upon to assist.

Excess outputs

Here we assume that $p > m$. In this case, we cannot hope to control each of the measured outputs independently at all times. We investigate three alternative strategies

(a) *Squaring down*

Although all the measurements should be used in obtaining state estimates, only m quantities can be independently controlled. Thus, any part of the controller that depends on state-estimate feedback should use the full set of measurements; however, set-point injection should be carried out only for a subset of m variables.

(b) *Soft sharing control*

If one really wants to control more variables than there exist inputs, then it is possible to define their relative importance by using a suitable performance index. For example, one might use a quadratic performance index.

(c) *Switching strategies*

It is also possible to take care of m variables at any one time by use of a switching law. This law might include time-division multiplexing or some more sophisticated decision structure.

The availability of extra inputs or outputs can also be very beneficial in allowing one to achieve a satisfactory design in the face of fundamental performance limitations. We illustrate by an example.

Example 24.3:

Inverted pendulum.

We recall the inverted-pendulum problem discussed in Example 9.4.

Example of an Inverted Pendulum

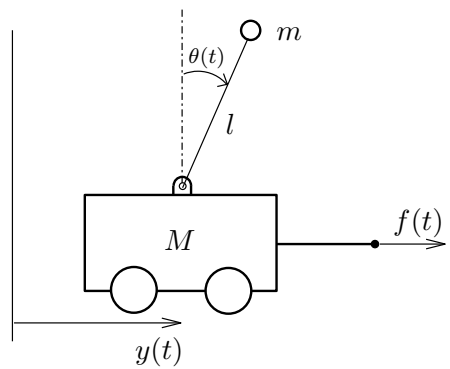

Figure 9.4: *Inverted pendulum*

We saw earlier that this system, when considered as a single-input (*force applied to the cart*), single-output (*cart position*) problem, has a real RHP pole that has a larger magnitude than a real RHP zero. This leads to a near impossible control system design problem. Thus, although this problem is, formally, controllable, it was argued that this set-up, when viewed in the light of fundamental performance limitations, is practically impossible to control, on account of severe and unavoidable sensitivity peaks.

However, the situation changes dramatically if we also measure the angle of the pendulum. This leads to a single input (*force*) and two outputs (*cart position*, $y(t)$, *and angle*, $\theta(t)$). This system can be represented in block-diagram form as on the next slide.

Figure 24.8: *One-input, two-output inverted-pendulum model*

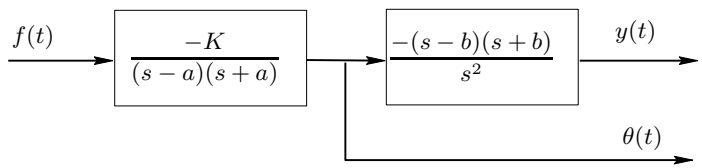

Note that this nonsquare system has poles at (0, 0, a, -a) but no finite (*MIMO*) zeros. Thus, one might reasonably expect that the very severe limitations which existed for the SISO system no longer apply to this nonsquare system.

We use $K = 2$, $a = \sqrt{20}$, and $b = \sqrt{10}$. Then a suitable *nonsquare* controller turns out to be

$$U(s) = \begin{bmatrix} C_y(s) & C_\theta(s) \end{bmatrix} \begin{bmatrix} R(s) - Y(s) \\ -\Theta(s) \end{bmatrix}$$

where $R(s) = \mathcal{L}[r(t)]$ is the reference for the cart position, and

$$C_y(s) = -\frac{4(s + 0.2)}{s + 5}; \qquad C_\theta(s) = -\frac{150(s + 4)}{s + 30}$$

The next slide shows the response of the closed-loop system for $r(t) = \mu(t\text{-}1)$, i.e., a unit step reference applied at $t = 1$.

Figure 24.9: *Step response in a nonsquare control for the inverted pendulum*

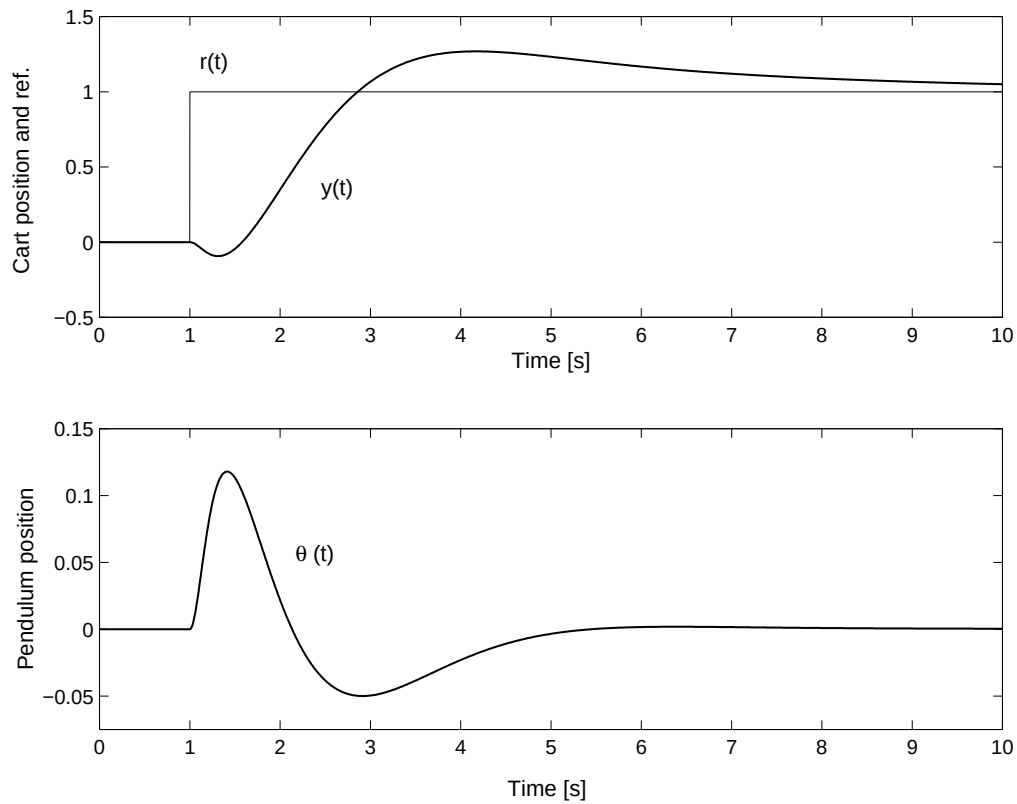

Note that these results are entirely satisfactory. An interesting observation is that the nonminimum-phase zero lies between the input and $y(t)$. Thus, irrespective of how the input is chosen, the performance limitations due to that zero remain. For example, we have for a unit reference step that

$$\int_0^\infty [r(t) - y(t)]\, e^{-bt} dt = \frac{1}{b}$$

In particular, the presence of the nonminimum-phase zero places an upper limit on the closed-loop bandwidth irrespective of the availability of the measurement of the angle.

The key issue that explains the advantage of using nonsquare control in this case is that the second controller effectively shifts the unstable pole to the stability region. Thus there is no longer a conflict between a small NMP zero and a large unstable pole, and we need only to pay attention to the bandwidth limitations introduced by the NMP zero.

Summary

- Analogously to the SISO case, MIMO performance specifications can generally not be addressed independently from another, because they are linked by a web of trade-offs.
- A number of the SISO fundamental algebraic laws of trade-off generalize rather directly to the MIMO case:
  - $\mathbf{S_o}(s) = \mathbf{I} - \mathbf{T_o}(s)$, implying a trade-off between speed of response to a change in reference or rejecting disturbances ($\mathbf{S_o}(s)$ *small*) versus necessary control effort, sensitivity to measurement noise, or modeling errors ($\mathbf{T_o}(s)$ *small*);
  - $Y_m(s) = -\mathbf{T_o}(s)D_m(s)$, implying a trade-off between the bandwidth of the complementary sensitivity and sensitivity to measurement noise.

- $\mathbf{S_{uo}}(s) = [\mathbf{G_o}(s)]^{-1}\mathbf{T}_o(s)$, implying that a complementary sensitivity with bandwidth significantly higher than the open loop will generate large control signals;
- $\mathbf{S_{io}}(s) = \mathbf{S_o}(s)\mathbf{G_o}(s)$, implying a trade-off between input and output disturbances; and
- $\mathbf{S}(s) = \mathbf{S_o}(s)\mathbf{S}_\Delta(s) = [\mathbf{I} + \mathbf{G}_{\Delta\mathbf{1}}(s)\mathbf{T_o}(s)]^{-1}$, implying a trade-off between the complementary sensitivity and robustness to modeling errors.

- There also exist frequency- and time-domain trade-offs due to unstable poles and zeros.
  - *Qualitatively*, they parallel the SISO results in that (*in a MIMO measure*) low bandwidth in conjunction with unstable poles is associated with increasing overshoot, whereas high bandwidth in conjunction with unstable zeros is associated with increasing undershoot.
  - *Quantitatively*, the measure in which the above is true is more complex than in the SISO case: the effects of under- and overshoot, as well as of integral constraints, pertain to linear combinations of the MIMO channels.

- MIMO systems are subject to the additional design specification of desired degree of decoupling.
- Decoupling is related to the time- and frequency-domain constraints via directionality.
  - The constraints due to open-loop NMP zeros with noncanonical directions can be isolated in a subset of outputs, if triangular decoupling is acceptable.
  - Alternatively, if dynamic decoupling is enforced, the constraint is dispersed over several channels.
- Advantages and disadvantages of completely decentralized control, full diagonal dynamical and triangular decoupling designs were illustrated with an industrial case study.